Rapid prototyping of cyclic olefin copolymer (COC) microfluidic devices

S. Ali Aghvami[a], Achini Opathalage[a], Z.K. Zhang[b], Markus Ludwig[a],
Michael Heymann[a,c,d], Michael Norton[a], Niya Wilkins[e], Seth Fraden[a,*]

[a] Martin Fisher School of Physics, Brandeis University, Waltham, MA, 02454, USA
[b] Key Laboratory of Functional Polymer Materials of Ministry of Education, Institute of Polymer Chemistry, College of Chemistry, Nankai University, Tianjin 300071, China
[c] Current address: Max Planck Institute of Biochemistry, Martinsried, 82152, Germany
[d] Graduate Program in Biophysics and Structural Biology, Brandeis University, Waltham, MA 02454, USA
[e] NanoHU, School of Science, Hampton University, Hampton, VA 23668, USA

ABSTRACT

We introduce a low-cost, high yield rapid fabrication method for casting COC microfluidic chips that is appropriate for academic labs and small companies. Devices are comprised of two molded pieces joined together to create a sealed device. The first piece contains the microfluidic features and the second contains the inlet and outlet manifold, a frame for rigidity and a viewing window. The microfluidic features are patterned using a PDMS mold that itself was replica-molded from a photoresist master. Dimensional stability of the microfluidics portion of the COC device is achieved by confining the PDMS mold in an aluminium frame. The mold for the lid is CNC milled from aluminium. Sealing the COC device is accomplished by timed immersion of the lid in a mixture of volatile and non-volatile solvents followed by application of heat and pressure. Surface treatment to render the device fluorophilic is performed using dopamine in assembled devices.

© 2017 Elsevier B.V. All rights reserved.

1. Introduction

The great majority of microfluidic devices fabricated in academic settings are made from the elastomer PDMS because the suite of processing steps known collectively as *soft lithography* [1] consisting of (1) master creation in photoresist, (2) molding in PDMS, (3) sealing and (4) fluidic interfacing are robust, simple and inexpensive [2]. However, PDMS has its drawbacks including permeation by water and organic solvents, swelling in organic solvents, softness, rapid restructuring of molecules located at the surface which degrades surface treatments, and high manufacturing costs which limits commercialization of microfluidic devices based on PDMS. The aim of this paper is to adapt soft lithography to the manufacturing of thermoplastic microfluidics while retaining the reliability, ease and low cost of processing PDMS.

In comparison to PDMS, thermoplastics offer increased solvent resistance, higher rigidity and low cost of mass production. Although over the past 15 years there have been a number of

publications describing rapid prototyping of thermoplastics, the methods have not been widely adopted in academic settings [3–22]. This article is targeted towards those research academic labs and small companies which lack the full bevy of thermoplastic manufacturing equipment and have the need for rapid prototyping of thermoplastic microfluidics. One reason why relatively few academic research labs produce thermoplastic microfluidics is that prior publications addressed individual processing steps, without focusing on the integration of all the steps needed to reliably, rapidly and economically fabricate functional thermoplastic microfluidic devices. Here we describe an inexpensive method for rapid prototyping of thermoplastic microfluidics that is designed for academic labs that need devices in a more rigid and/or more solvent resistant material than PDMS, need to treat the surface, or want to manufacture a pre-commercial thermoplastic version of a microfluidic device in order to demonstrate the potential to mass produce the prototype, which will facilitate the transfer of academic developed technology to commercialization. We focus on the thermoplastic COC (Cyclic Olefin Copolymer) which has been widely used in commercial applications, but less so in the academic labs. In the body of this paper we describe the process to produce a thermoplastic device, how to surface treat the assembled devices

* Corresponding author.
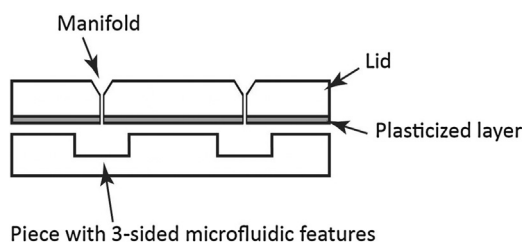 *E-mail address:* fraden@brandeis.edu (S. Fraden).

Fig. 1. Schematic cross-section of a COC microfluidic device comprised of a 3-sided featured piece and a featureless piece, or lid, that contains a manifold. A thin layer of the lid is solvent plasticized in order to bond the pieces together.

to be hydrophilic or fluorophilic and describe the instrumentation needed to make a thermoplastic microfluidic device. Finally, we utilize the COC devices for two applications; protein crystallization and emulsion generation. In the Supplementary data we include the processing details, manufacturing instructions and a comprehensive series of videos demonstrating each of the process steps. The focus of this article is not on developing new methods, but on refining and combining many existing processes to present a simple, yet complete and robust soft-lithography based process to produce microfluidics in COC.

2. Process overview

The microfluidic device is comprised of two COC pieces. The first contains the microfluidic features consisting of 3-sided open channels and wells that are cast in the COC. The second is the "lid" which seals the 3-sided microfluidics and contains a manifold with conical ports to connect the inlet/outlet tubing for loading the microfluidic device (Fig. 1). The microfluidic piece is fabricated by first creating a photoresist master and then casting a PDMS replica, just as in normal soft lithography. In contrast to soft lithography, we employ the PDMS replica as a mold to cast the thermoplastic device from molten COC. The lid is fabricated by CNC milling an aluminium mold from which the COC lid is directly embossed. The two thermoplastic pieces are bonded together using a combination of chemical, thermal and pressure bonding. Important design considerations are incorporation of a quick-connect, leak-free and high-pressure manifold for the inlets and outlets on the lid and registration marks that allow the precise alignment of the inlets and outlets located on the lid with the other COC piece containing the microfluidic features. Finally, the interior channels are treated to render the surfaces either oleophilic, fluorophilic or hydrophilic. All chips were manufactured using TOPAS 8007, which has a glass temperature of 78C and a melting temperature of 190C (see Supplemental data – COC pellets specification).

2.1. Photoresist master

The photoresist master containing the microfluidic features is constructed using the established methods of soft lithography [1]. We design the photomask in Auto-Cad (AutoDesk Inc.) and purchase a film photomask from (Cad/Art services, Inc.). A spincoater (PWM32 – Headway Research, Inc.) is used to apply negative photoresist (SU8-3010, Microchem Inc.) on a 3-inch silicon wafer (Silicon Sense Inc.) and the pattern is exposed using a mask aligner (ABM, Inc.). This procedure is shown in Supplemental Data MovieS1. All of our devices are designed to be a standard size, which we have arbitrarily picked to be 3 cm by 4 cm. In order to facilitate alignment of the top and bottom pieces, the only photoresist left on the wafer after development is a 3 cm × 4 cm zone and the rest of the wafer is bare silicon. This leaves a raised rectangular edge of photoresist whose purpose is to facilitate alignment of a plexyglass
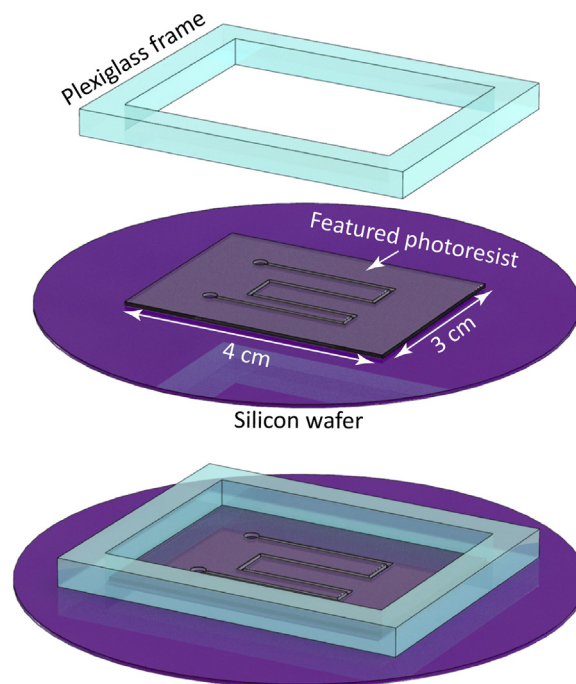

Fig. 2. Schematic of a silicon wafer and CNC milled plexiglass frame which seats snugly around the raised photoresist. Together, the frame and photoresist constitute the mold for a PDMS replica.

frame for casting of a PDMS mold described in the next section and illustrated in Fig. 2.

2.2. PDMS mold for microfluidic features

Photoresist deposited on silicon wafers have been used to directly transfer features to COC using a thermopress [15]. However, in spite of treating the photoresist surface with release agents, difficulties in separating the COC from the photoresist mold remain and the mold deteriorates rapidly [15]. Therefore, we transfer the microfluidic features from the rigid photoresist master into a soft elastomer, PDMS, which will be used to mold the thermoplastic. In contrast to photoresist, the elastic nature of PDMS makes demolding easy and reliable because the PDMS thins in the directions perpendicular to the direction it is stretched [4,10]. Additionally, PDMS is tough and

does not tear easily. Consequently, on the device described here, with features on the scale of 20 μm and aspect ratios around one, we have not noticed any deterioration of the PDMS mold after 100 cycles of molding.

To create the PDMS mold, the uncured PDMS is mixed in a 10:1 ratio by mass, degassed in a mixer (AR-250, Thinky Co.) and poured into a plexyglass frame, which is temporarily sealed to the photoresist master with a small amount of vacuum grease. The inside of the frame precisely aligns against the 3 cm × 4 cm raised photoresist. A glass slide is placed on top of the plexyglass frame and clamped after making sure that the PDMS completely fills the plexyglass frame without any air bubbles. The purpose of this step is to prescribe the thickness of the PDMS and its alignment to the photoresist features. The PDMS is then placed in vacuum for about 20 min, and finally cured in an oven at 80° C for more than 2 h. For more detail refer to the Supplemental Data MovieS2.

2.2.1. CNC mill and laser cutter

To make the plexyglass frame, we used a hobbyist CNC mill, costing under $3k, from Sherline (2000 CNC, Sherline Products Inc.) and a laser cutter (MEL-40, Full Spectrum Laser LLC.), costing $3k. This
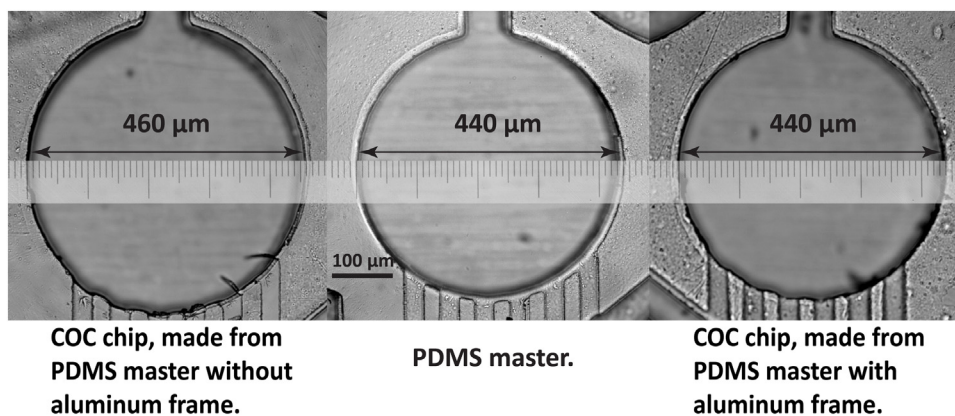
Fig. 3. Fidelity of reproduction. (a) COC chip thermoembossed from PDMS master without aluminium frame. The embossed features are larger than the mold. (b) PDMS master. (c) COC chip molded from PDMS with aluminium frame reproduces faithfully.

mill has poor performance characteristics, such as a maximum mill rotation rate of 2800 RPM and 50 μm backlash on the XY translation, but nevertheless, these specifications are adequate for making all the components described in this paper. The Sherline mill can run Mach 2/3, an easy to use and excellent CNC mill controller. Additionally, to design the piece and generate the G-code to operate the CNC we use a simple, inexpensive CAD/CAM program, Cut2D (Vectric Ltd.). Mastering Cut2D takes a short time and although the functionality is greatly less than the industry standard, SolidWorks (Dassault Systèmes), so is the cost and ease of use.

We note that there are other newer options to the Sherline mill costing about $3k but with better specifications, such as produced by Carbide 3D and Other Machine Co. The inexpensive laser cutter we use is not adequate for making microfluidic devices directly as the smallest channel width is approximately 1 mm. However, it works well for making auxiliary parts, such as frames for clamping microfluidic elements or molds for casting large components.

Both the laser cutter and CNC mill, costing a total of $6k, have greatly increased the productivity of microfluidics in our lab [23]. The cutter and mill are housed in the main lab, outside the cleanroom. Ease of access to the equipment, along with the ease of the software used to design parts and operate the equipment, are important for adoption by students. With only a minimal of machine shop training students are able to manufacture a wide range of parts that previously required outsourcing to the university machine shop, which was both more costly and time consuming.

2.3. Thermal forming of COC microfluidics

We employed thermo-embossing in a first attempt at transferring features from PDMS to COC [18]. During thermal embossing a sheet of thermal plastic is heated to temperatures above its glass temperature, but below its melting temperature. Then, using a pneumatic press, the heated, soft COC sheet is pressed into the soft PDMS mold, which has the form of a rectangular slab.

As reported in the literature, the features on the mold are embossed into the COC sheet, but what wasn't reported was that the mold is also compressed in the direction normal to the slab and expands in the other two directions. This pressure-driven expansion changes the dimensions of the entire device (Fig. 3). One way to solve this issue is to make a rigid epoxy replica of the photoresist [12]. However, demolding the epoxy from the photoresist, as well as demolding the COC from the epoxy is more difficult than demolding photoresist and COC from flexible PDMS.

In order to use PDMS as a mold while transferring the features of the PDMS mold to the COC with fidelity, we CNC machined an
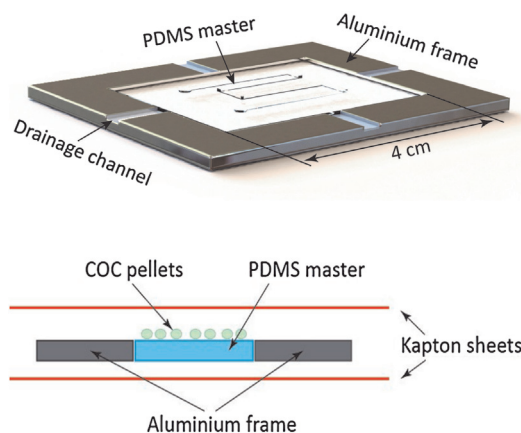

Fig. 4. Schematic of casting assembly for molding patterned COC starting with COC pellets. Fabrication of PDMS master is done prior to this step as shown in Fig. 2.

aluminium frame that fit precisely around the PDMS master as shown in Fig. 4. The aluminium frame (3 mm height), which has the same dimensions as the frame in Fig. 2, constrains the PDMS from expanding in the directions perpendicular to the axis of compression. Moreover, to reduce the compression of the PDMS we raised the temperature of the COC to 150C, high above its glass temperature. The melting temperature of COC is broad due to polymer polydispersity. We also made chips at several temperatures between 150C and 200C. The trend was that the longer the chip is under pressure and the higher the temperature, the thinner the final chip without any other obvious difference in the final result. These results are consistent with the known temperature dependence of the viscosity of COC, which decreases with increasing temperature. An advantage of processing at higher temperatures is an increase in speed due to lowered viscosity. However, at 200C the Kapton sheets stick more to the COC and after 100 cycles the PDMS turns yellow and becomes brittle. We machined drainage channels into the aluminium frame so that the softened COC could squeeze out of the frame in an attempt to relieve excess pressure on the PDMS. Therefore, this processing method shares features with molten casting and is distinct from thermo embossing because the thermoplastic is processed in a molten state. Using this casting method we faithfully reproduced all of the features in the PDMS mold within the experimental accuracy of 1 μm in all three dimensions as shown in Fig. 3.

The thickness of the featured COC sheet was about 100 μm. During processing, the molten COC spread over the PDMS master and
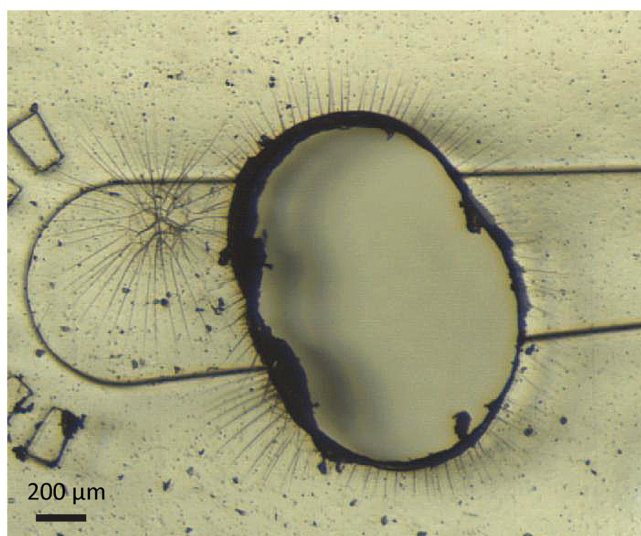
Fig. 5. Cracks appear when an access hole is drilled after thermoembossing a commercial COC sheet.

Fig. 6. Schematic of COC lid, constructed in one piece, but comprised of three different elements, each with a different thickness.

aluminium frame so that the lateral dimensions of the COC sheet exceeded the size of the PDMS master. However, the boundary of the aluminium frame and PDMS master left a thin mark clearly delineating the boundary, which we used as a guide to easily cut the sheet to the 3 cm x 4 cm size of the PDMS master using scissors.

Besides eliminating distortion of the PDMS master, processing the COC in the molten state has two more advantages over thermo embossing. One is that we use COC pellets (Grade 8007, TOPAS) for the stock material instead of hot embossing commercial COC sheets (F10-21-1, TOPAS 8007), which is economical as pellets are much less expensive than sheets. A second advantage is that COC microfluidic devices cast from pellets performed significantly better than COC devices formed from thermo embossing thin commercial sheets of thicknesses in the range of 50 μm – 150 μm. The difference was the appearance of cracks and crazing around holes drilled into the commercial COC sheets for inlet and outlet connections (Fig. 5), while there was an absence of crazing in COC sheets of the same thickness and molecular weight, but freshly formed from melting COC pellets. Therefore, it is not thermo embossing per se that leads to crazing, but crazing occurs because of a difference in the stock material itself. It is probable that commercial thin sheets are manufactured by extrusion, which builds in residue stress, leading to the crazing. It is noteworthy that thicker commercial COC plates of thickness 1 mm or greater showed no crazing upon drilling. The thicker plates were likely produced by casting, which results in smaller residual stress than extrusion. Details of producing thin sheets from pellets are given in the Supplemental Data (Table S1, MovieS3).

To obtain a clear surface finish on the COC device and prevent the molten COC from sticking to the thermo press, we place a piece of Kapton sheet (American Durafilm Kapton Film, 5 MIL) on top of the pellets. A drawing of the confined PDMS master mold, ready for the casting of COC, is shown in Fig. 4.

2.3.1. Thermo press

Our thermo press is home-made, but based on a commercial pneumatic press (DAP38, Air-Mite, Inc.), which was modified to include two heaters, one cooling block, a load gauge, a digitally controlled regulator and interfaced with LabVIEW (National Instruments). The thermo press design was based on previously published work and can produce significantly higher forces and temperatures than needed for COC casting and lidding [24].
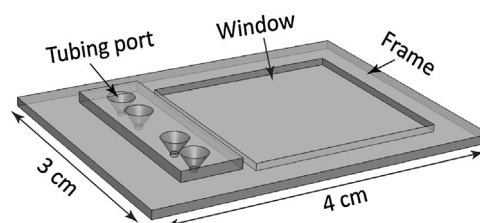
To promote wide spread adoption of thermoplastic processing by the academic community there should be an inexpensive commercial source of a thermo press optimized for thermoplastic microfluidics. A thermo press suitable for rapid prototyping would generate forces between 10 and 1000N (2–200 lbs) and temperatures up to 250C. It would include high power heaters and cooling elements to speed up processing times, with a working area of 15 cm × 15 cm. The duration, pressure and temperature of the thermo press should be programmable and it is important to monitor the pressure and temperature of the thermoplastic.

2.4. Aluminum mold for lid

In our design the "lid" (Fig. 6) is the piece of thermoplastic that is used to bond to the piece of thermoplastic that contains the 3-sided microfluidic features described in the previous section (Fig. 1). In the simplest configuration the lid is a featureless sheet of COC. However, we added several features to the lid to increase the functionality of the microfluidic device (Fig. 6). One of the major difficulties in microfluidic chip design is the "world-to-chip" problem, or interface between the microfluidics and external plumbing, which we address by integrating a manifold that bridges the gap between macro scale external tubing and microfluidic channels in the chip[20]. For added convenience our manifold is designed to allow rapid, reliable and reversible connecting and disconnecting of tubing to the sealed chip. Our concept is that we make one lid that can be used in a large number of microfluidic designs, but where each chip has the same inlet and outlet connections. The decision to place 4 ports on the lid was arbitrary; it's a convenient number that works for most applications in our lab. For applications that require fewer than 4 ports, the extra ports are simply unused. We designed a manifold with flat-bottomed ports using Cut2D and we designed a manifold with a cone-bottomed port using SolidWorks and SolidCAM. We also machined molds for PDMS ferrules to fit into the manifold, shown in Fig. S3 in the Supplemental Data. Additionally, one of our applications requires a thin window of order 100 μm thickness in order to have x-rays pass through the sample with minimal scattering and to have optical clarity. Consequently, the lid consists of three different areas with different functions and thicknesses; an inlet/outlet manifold with tubing ports, a frame for mechanical support, and a thin observation window. To facilitate manufacturing, all are cast in one piece. One side of the lid is completely featureless and flat. This side is used to seal the microfluidics and other side contains the plumbing manifold, support frame and observation window.

We CNC machined the mold for the lid out of aluminium. To facilitate demolding we constructed the aluminium mold in two layers (Fig. 7). This form of mold construction is important in order to facilitate demolding. We were unable to demold the COC when the mold was one piece. Applying a layer of thin Kapton tape on the window area of aluminium mold is necessary to obtain a clear transparent finish on the window section of the lid.

The aluminium mold is placed inside an aluminium frame and COC pellets are poured on top of the aluminium mold. A piece of
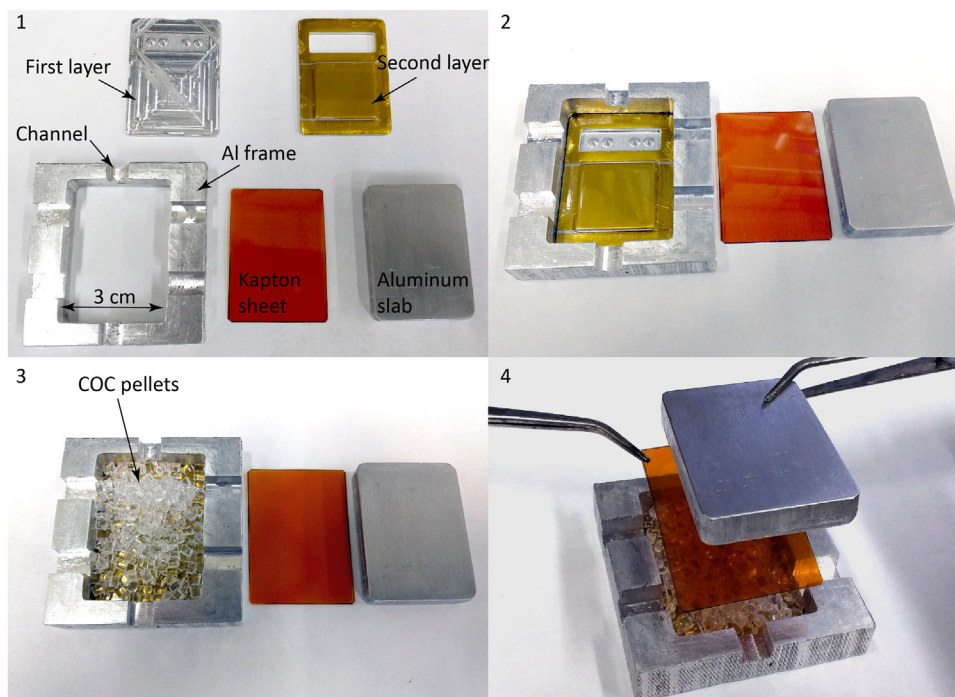
Fig. 7. CNC machined aluminium mold for making the COC lid. (1) The second aluminium layer is Kapton taped so demolding will be easier and the surface finish will be transparent. (2) The two layer mold is placed in the aluminium frame. (3) COC pellets are loaded in the mold. (4) A sheet of Kapton is first placed on top of the pellets followed by placement of the aluminium slab. The assembly is ready for applying heat and pressure.

Kapton sheet is placed on top of the COC pellets and then a small aluminium slab is placed on top of the Kapton sheet. The assemblage is placed in the thermo-press, heated above the COC melting temperature, and then pressure is applied as specified in Supplemental Data Table S2 and MovieS4. The frame contains drainage channels for the excess COC to flow out.

2.5. Sealing the chip

We use a solvent bonding method, which seals the featured and non-featured COC pieces with low distortion and high strength [7]. The bonding method has two steps; first solvent treatment followed by application of heat and temperature. In the solvent treatment step, the COC lid is soaked in a mixture of ethanol-decalin, 85–15% by weight for 5 min. The aim of the solvent treatment is to produce a thin layer of plasticized COC that acts like a glue for bonding the COC cover to the featured COC. The ethanol-decalin ratio was optimized. At higher decalin ratios there was significant fill-in of channels, while for lower decalin ratios the bonding was weak.

This method has been described as type-II diffusion in which the diffusion constant of the solvent is a function of the degree of swelling of the plastic [25]. This leads to non-linearity in the diffusion equation and produces an abrupt interface between the swollen and non-swollen thermoplastic that advances into the plastic at a constant velocity. However, when we measured the increase in weight as a function of soaking time and compared with theory, we found that our measurements were inconsistent with type-II diffusion and instead was better fit assuming a constant value of the diffusion constant, as shown in Fig. 8a.

To perform the mass uptake measurements, we immersed a freshly made rectangular slab of COC of dimensions 30 mm by 40 mm by 1 mm with a dry weight of 2 g. The slab was immersed in the fluid for a time interval, then removed, dried using compressed air and weighed. To perform the evaporation rate measurements, we removed the COC slab from the ethanol-decalin bath after an interval of immersion, rinsed the slab with ethanol, dried using compressed air and weighed the COC slab as a function of time.

We found that the uptake and release rates of solvent were different, with uptake occurring at a much faster rate than the release of solvent as shown in Fig. 8. We computed rates using a model that treated the solvent as a 1-component fluid [26]. This model predicted that the absorption and desorption rates would be the same, in contradiction with experiment. The discrepancies between our work and previous work [7] and between the model and experiment deserve further attention. However, the fact that the desorption is slow means that the sealing procedure is insensitive to how long the sealing process takes, which is a great advantage for manufacturing microfluidic devices.

We also manufactured a "stability form" from PDMS whose function is to prevent distortion of the lid during the sealing process. To make the stability form we use the COC lid itself as a mold to make a complimentary shape in PDMS. Inserting the PDMS stability form into the complimentary COC lid results in a structure in which all the indentations in the COC lid are filled, creating a solid rectangular block with horizontal flat surfaces. We then align the featured and un-featured solvent treated pieces of COC, place a slab of PDMS to distribute the stress uniformly and insert the combination in the thermal press (Fig. 9). Next we raise the temperature to several degrees below the glass temperature and apply pressure as specified in the Supplemental Data Table S3, MovieS5.

We measured the height of features on the COC before and after sealing and determined that after sealing there was a 3–4 μm loss in height. There are alternate methods to seal thermoplastics that do not lead to filling in of channels. A method for bonding two dissimilar thermoplastics has been reported to seal a device in which the channels were nanometeres in height, but did not work for bonding COC to COC [21]. Silane coupling agents, which should have no filling in of channels, have been used to seal COC to PDMS [9,14], but when we applied this silane method to seal COC to COC we found that the bonding strength was unacceptably low. We are unaware of any covalent bonding method for bonding COC to COC.
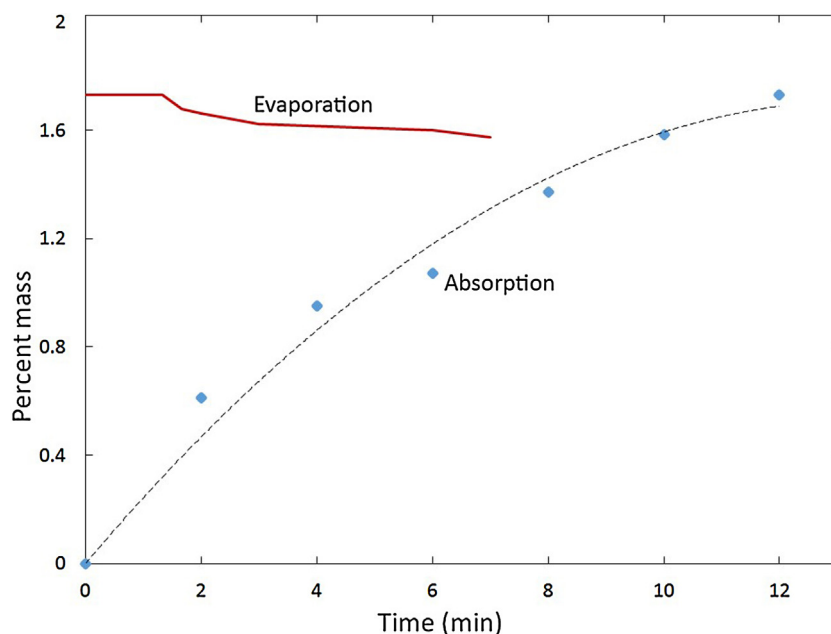
Fig. 8. Measured mass uptake and evaporation rates of a COC block. which has been immersed in an ethanol-decalin, 85–15% by weight mixture. Dashed curve is theory assuming a constant value of the diffusion constant.
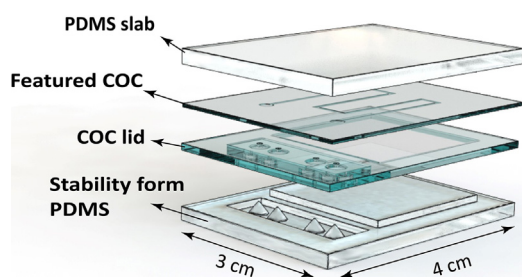

Fig. 9. The orientation of COC and PDMS pieces during the sealing procedure.

The sealed chips were pressurized up to 250 PSI without any evidence of delamination. Above 250 PSI the connectors leaked (described below), which prevented testing delamination at higher pressures.

2.6. Surface treatment

The surface energy of COC is low, 30 dyn/cm (Grade 8007, TOPAS). Consequently, fluorinated oils have a low contact angle, hydrogenated oils wet and even dissolve COC, and water has a contact angle with COC that is close to 90°. One important category of microfluidic applications is making emulsions. In order to make emulsions with COC devices it is necessary to control the surface chemistry and ideally render the surface either fluorophilic, hydrophilic, or oleophilic depending on which continuous phase is desired. The signature of wetting is the appearance of thick, smooth black lines at the air-COC interface in bright field microscopy indicating the fluid (water or oil) wets the COC, as shown for water and surfactant in Fig. 10b. No black lines at the air-COC interface are present for water alone, shown in Fig. 10a indicating that water does not wet COC. Without any surface treatment water does not wet the COC surface, however, with 3% Triton surfactant, water does wet the untreated COC. Mineral oil, with and without surfactant wets COC (Fig. 10c and d), while fluorinated oil, with and without surfactant, partially wets the COC surface as shown in Fig. 10e and f.

Rendering the COC surface fluorophilic is a two-step process. The COC was first treated with Dopamine hydrochloride (H8502 Sigma) in basic Tris buffer, which produces a hydrophilic poly-dopamine (PDA) coating via oxidation induced self-polymerization of dopamine [27], as shown in step 1 of Fig. 10g. Water wets the PDA treated COC surface as shown by the dark meniscus at the air-COC interface in Fig. 10h. As a surface treatment PDA has two virtues; a propensity to stick to a wide variety of surfaces and high chemical reactivity [28]. The treatment process consists of flowing dopamine, prepared to be $2 \, \text{mg} \, \text{mL}^{-1}$ in Tris buffer (20 mM with pH = 8.5), through the assembled device at 500 µl/hr for 2 h. With time, the Dopamine hydrochloride polymerizes into PDA and deposits on the internal surface. PDA is dark and darkens with increasing thickness of the coating, so care is taken not to deposit too much. Once the deposition is completed, the device is rinsed with ethanol and dried with compressed nitrogen. Next a solution of 1H,1H,2H,2H-perfluorodecanethiol in ethanol with a concentration of $50 \, \text{mg} \, \text{mL}^{-1}$ was flowed through the device at 100 µl/hr for 2 h, as shown in the step 2 of Fig. 10g, after which the device was rinsed again with ethanol. The −SH group of perfluorodecanethiol reacts with the polydopamine coating and renders the surface fluorophilic as shown by the dark meniscus at the air-COC interface in Fig. 10i. We did not optimize the degree of fluoridisation of the channels.

2.7. Fluidic interface

For connecting the tubing to the chip, we built a simple frame to hold the microfluidic device and manufactured a PDMS ferrule for the 1/32" tubing. The PDMS ferrule is inserted into the cone shaped port on the COC manifold and the tubing is inserted, as shown in Fig. 11. The manufacturing of the ferrule is described in the supplement (Fig. S3). Once properly sealed, the device operated without leaking for pressures up to 250 psi for both the flat-bottomed and cone-bottomed ports. The cone-bottomed ports sealed with 100% reliability. The flat-bottomed ports were less reliable. About 50% of the time, they leaked for all pressures, but when they did seal, they didn't leak until 250 psi.
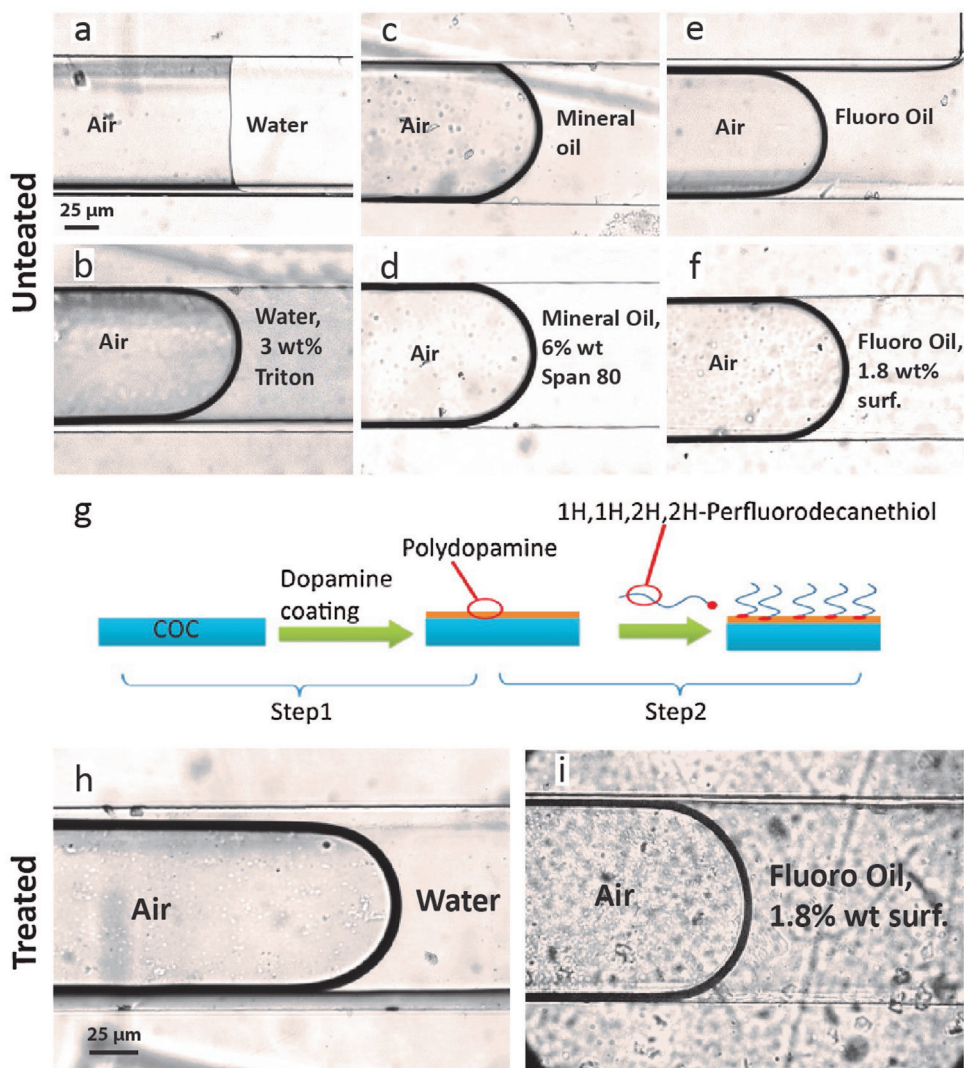
Fig. 10. Characterizing untreated COC channels (a-f), performing surface treatments (g) and characterizing treated COC channels (h, i). (a) Air/water interface (b) Air/water in Triton (c) Air/Mineral oil interface (d) Air/Mineral oil in Span 80 interface (e) Air/HFE7500 (f) Air/HFE7500 containing PFPE-PEG-PFPE surfactant from RAN Biotechnologies (g) Two-step surface treatment to render COC fluorophilic. (h) Water wets the PDA coated COC after step 1. (i) Fluorinated oil/surfactant wets the COC channel after step 2.
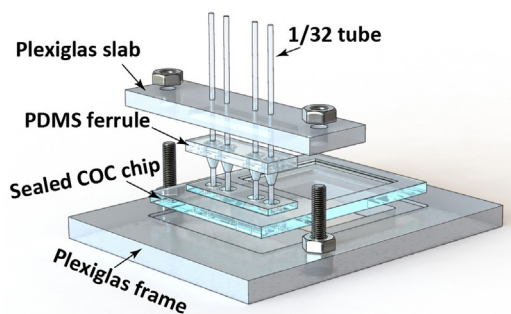

Fig. 11. Simple jig for loading fluidics into device.

We did not optimize the connections as 250 psi was a greater pressure than needed for any of our applications. We assume higher sealing pressures could be achieved with more rigid materials, such as PEEK, for the tubing and ferrules.

2.7.1. Application examples and discussion

We tested the rapid prototyping of thermoplastic microfluidics method by producing devices for two different applications: (1) a device for generating and storing drops based on capillary valves, the so-called "store then create" design[29], which we have used for protein crystallization [14] (Fig. 12), and (2) a drop generation chip using flow-focusing to make emulsions [30].

2.7.2. Application 1 – protein crystallization

Here we crystallize protein in a COC chip, which is illustrated in Fig. 12a. In operation, the device consists of 200 wells filled with lysozyme and isolated by fluorinated oil. Isolation is created by capillary valves located at the entrance and exit of each well. In order for the capillary valves to operate with fluorinated oil it is required that the COC surface be fluorophillic. This chip is a variant of the store-then-create design [29], which we have modified to include valves of different heights. Multi-height valves are a significant improvement over the previous design because they allow a greater range of opening pressures, which makes operation more robust. In our prior design, the capillary valves were tall and thin [29]. Such high aspect ratio structures in photoresist are fragile and this was not a robust manufacturing design. Additionally, the use of a single narrow capillary valve resulted in a high fluidic resistance and consequently high pressure in the chip, which promotes leaks. The use of multi-height valves allows flipping the valves on their sides. The aspect ratio of the capillary valve remains the same,
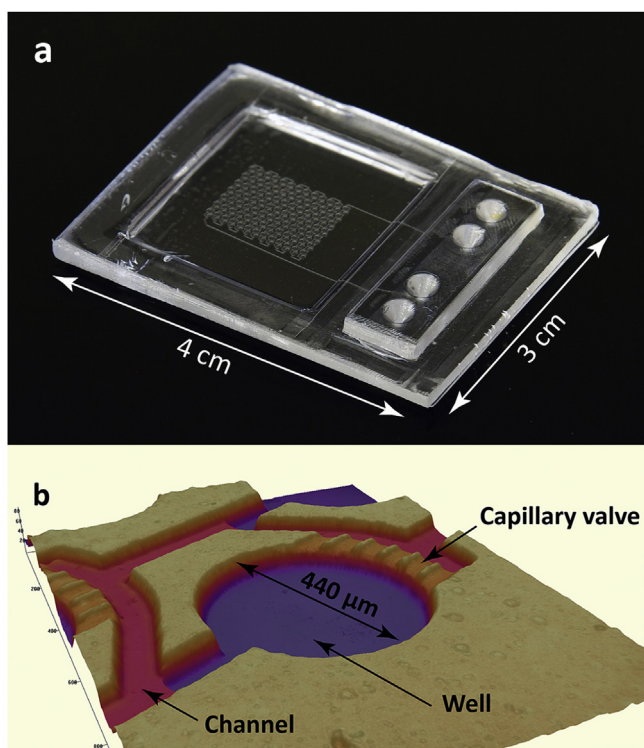
Fig. 12. Store then Create protein crystallization chip. a) Image of the assembled chip. Autocad design is provided in the Supplemental Data. b) Profilometer image of featured COC for protein crystallization. The design places 200 wells of 7.6 nL volume connected in series in a square centimeter. The design uses features of three different heights, with the main channel 25 μm, the wells, 50 μm, and the capillary valves, 12 μm height. Channels filled in 3–4 μm during the sealing process.

but the resulting structure in the photoresist is much more stable mechanically. We also installed six capillary valves in parallel. This lowered the hydrodynamic resistance by six without any decrease in the capillary valve break-out pressure.

The chip is designed with thin windows to allow on-chip x-ray diffraction of protein crystals [8,14,31]. For our purposes, the stringent requirements on the multi-height, high density microfluidic features and surface treatment of this chip provide a thorough test of our thermoplastic chip fabrication methods. This store-then-create chip consists of segments of three different heights, which on the PDMS master had the following dimensions: I) wells, which store the protein solution, that were 50 μm height and 440 μm diameter with a volume of 7.6 nl, II) channels with 25 μm height and 73 μm width III) exit capillary valves with 12 μm height and 30 μm width (Fig. 12b). As a model system we crystallized lysozyme protein from chicken egg white (Sigma). Each drop initially contained the mixture of 12.5 mg/ml of Lysozyme, 6.5% (w/v) PEG 8 kD and 2.5% (w/v) NaCl in 0.1 M of NaAC buffer at pH 4.8.

The piece of COC with the microfluidics was faithfully reproduced from the PDMS in all three dimensions within an accuracy of 1 μm. However, we observed that the channels filled in about 3–4 μm after bonding the lid to the COC piece with the microfluidics. The exit capillary valves, which were 12 μm in height before the lid was attached were 8 μm high after the lid was attached. Next, the assembled chip was fluorinated as described previously in Section 2.6.

To load the chip with protein, we used a 2 position, 6 port valve (LabSmith-MV303) in an injection loop configuration to avoid introducing any air bubbles and to precisely control the volume of protein, which in this case was 1.5 μl. Tubing was introduced into the chip via the manifold described in section 4. The first step in the

loading process is to fill the chip with oil. In practice, air is trapped in the device because the air-oil interface has a surface tension and can cause the capillary valves to retain the air. However, air has a high solubility in fluorinated oil and is rapidly absorbed because the chip is pressurized while the oil is being injected into the chip. In a few minutes the chip is completely filled with oil. The second step is to load the 1.5 μl of protein. The final step is injecting oil again, purging the protein from the channels and thereby isolating the contents of each well. A figure of the chip connected to the external plumbing is included in the supplement (Fig. S4 in Supplemental Data) and a movie showing the fluid loading process is included in the Supplemental Data MovieS6. All 200 capillary valves operated as designed with zero failures. Note that this design has zero dead volume; 100% of the sample ends up in the wells with no sample exiting the chip or residing in the channels, as shown in the Supplemental Data MovieS7. The nucleation rate and sample volumes were chosen to favour the formation of only one crystal per well, which is optimal for protein structure determination [32]. Crystals formed in each well in one of two polymorphs as shown in Fig. 13.

COC has a low value of water permeation with a vapour transmission rate of 0.028 g mm/m^2 day [33]. In contrast, PDMS has a hundred times greater water permeation rate. Drops in the device shown in Figs. 12 and 13 had windows of 100 μm thickness and took a month to evaporate to half of their original volume. In contrast, drops in a device of the same design, but constructed of PDMS with a window of 100 μm dry out in several hours.

2.7.3. Application 2 – flow-focussing droplet formation

There is great interest in droplet microfluidics [34] so we tested whether COC chips manufactured with our thermoplastic prototyping method could produce emulsions using the flow focusing design [10]. We began with untreated COC and sought to create three different emulsions. We first successfully generated emulsions of hydrogenated oil droplets in water. The continuous phase was water, the surfactant was Triton-X100 at 3% concentration, and the dispersed phase was n-hexadecane oil as shown in Fig. 14a. The second emulsion successfully generated was water droplets in hydrogenated oil. The continuous phase was light mineral oil, the surfactant was Span 80 at 6 wt% concentration and the dispersed phase was distilled water, as shown in Fig. 14b. We failed to generate a third emulsion consisting of water droplets in fluorinated oil with surfactant using untreated COC. We observed that the water stream wetted the upper and lower surfaces of the channel forming a jet that would not break up into drops as shown in Fig. 14c. We reasoned that if the COC was treated to be fluorophillic then the oil would wet the COC instead of the water and the water jet would become unstable and break into drops. This approach worked and using the perfluorodecanethiol surface treated device that was described previously in section 6, we were able to make water-in-fluorinated oil emulsions. The continuous phase was HFE-7500 (3 M Corp.) oil mixed with 1.8% surfactant which has an amphiphilic PFPE-PEG-PFPE fluorinated block copolymer (RAN Biotechnoloiges), similar to a surfactant described in literature [35]. The dispersed phase was distilled water, as shown in Fig. 14d.

3. Conclusion

We have demonstrated a complete, robust, cost-effective method for making thermoplastic microfluidic devices with integrated tubing ports by melting COC pellets in a PDMS mold. We improved upon previous methods by surrounding the PDMS mold with a rigid metal frame to prevent distortion of the PMDS. The chip was manufactured from two pieces of COC. To seal the pieces
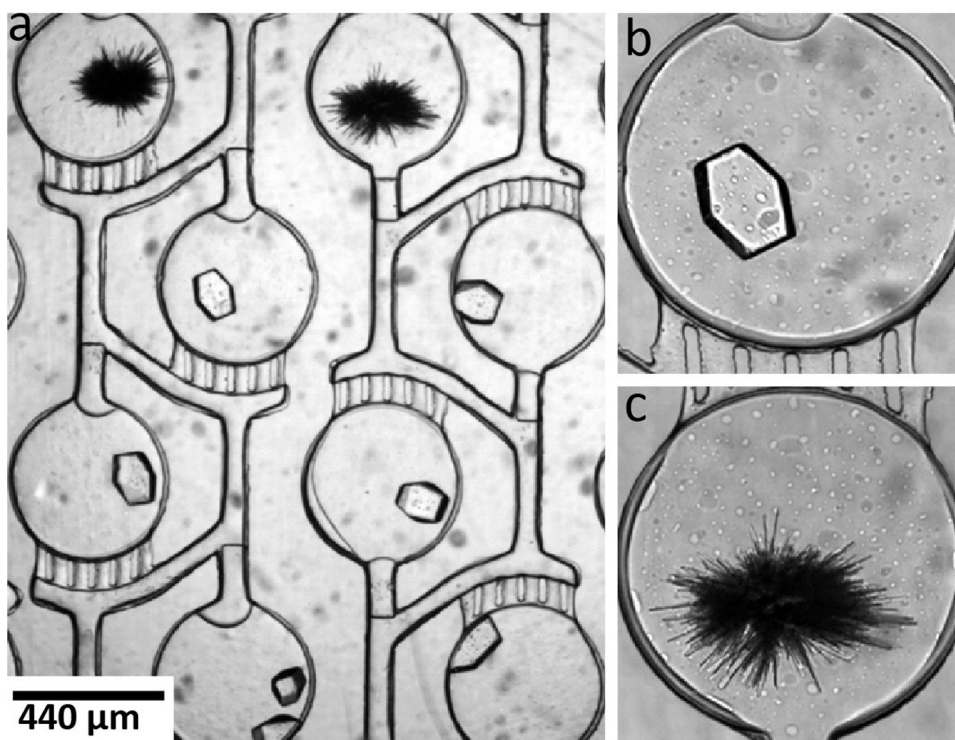
Fig. 13. Store then create-COC chip with 200 identical wells, all filled initially with the same supersaturated lysozyme solution. a) Protein crystals in two different polymorphs are observed. b) Tetragonal crystals. c) Spherulite crystals.
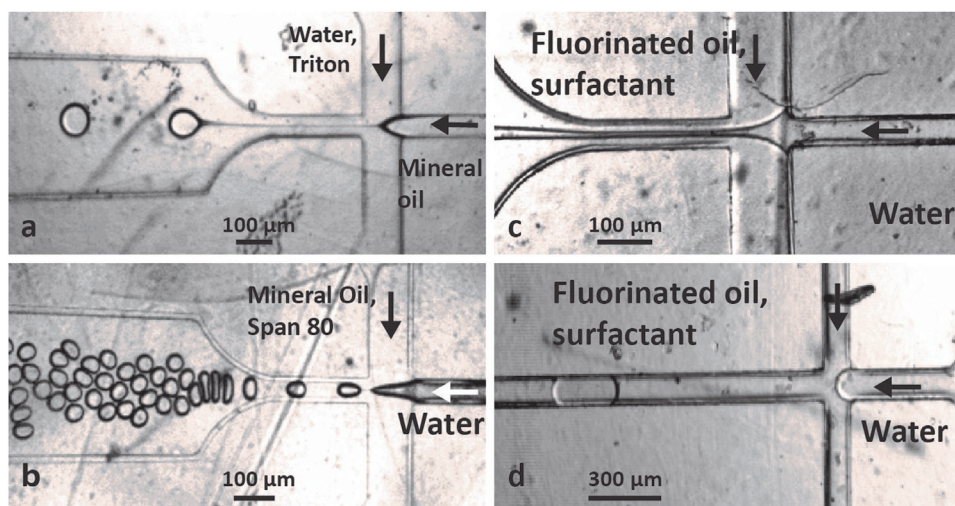

Fig. 14. Drop making in untreated and surface treated COC channels. (a), (b), (c) are not treated, (d) is treated. (a) Mineral oil in water, 3% Triton-x100 emulsion (b) Water in mineral oil, 6% Span 80 emulsion. (c) Jetting of water when fluorinated oil and surfactant is used as continuous phase. (d) Water in fluorinated oil and surfactant emulsion made in fluorinated COC drop-maker.

together, we first applied a solvent treatment to the lid and then applied heat and pressure to seal the lid to the piece containing microfluidic features. Comprehensive movies illustrating each of the processing steps and operation of the complete devices is included in the Supplemental Data. This method is suitable for rapid prototyping in academic labs and is useful for assessing whether a microfluidic device can be mass produced in thermoplastic.

Appendix A. Supplementary data

Supplementary data associated with this article can be found, in the online version, at http://dx.doi.org/10.1016/j.snb.2017.03.023.

References

[1] G.M. Whitesides, E. Ostuni, S. Takayama, X.Y. Jiang, D.E. Ingber, Annu. Rev. Biomed. Eng. 3 (2001) 335–373.

[2] J.C. McDonald, D.C. Duffy, J.R. Anderson, D.T. Chiu, H.K. Wu, O.J.A. Schueller, G.M. Whitesides, Electrophoresis 21 (2000) 27–40.

[3] H. Becker, L.E. Locascio, Talanta 56 (2002) 267–287.

[4] J. Narasimhan, I. Papautsky, J. Micromech. Microeng. 14 (2004) 96–103.

[5] B. Bilenberg, M. Hansen, D. Johansen, V. Ozkapici, C. Jeppesen, P. Szabo, I.M. Obieta, O. Arroyo, J.O. Tegenfeldt, A. Kristensen, J. Vacuum Sci. Technol. B 23 (2005) 2944–2949.

[6] D. Paul, A. Pallandre, S. Miserere, J. Weber, J.L. Viovy, Electrophoresis 28 (2007) 1115–1122.

[7] T.I. Wallow, A.M. Morales, B.A. Simmons, M.C. Hunter, K.L. Krafcik, L.A. Domeier, S.M. Sickafoose, K.D. Patel, A. Gardea, Lab Chip 7 (2007) 1825–1831.

[8] K. Dhouib, C.K. Malek, W. Pfleging, B. Gauthier-Manuel, R. Duffait, G. Thuillier, R. Ferrigno, L. Jacquamet, J. Ohana, J.L. Ferrer, A. Theobald-Dietrich, R. Giege, B. Lorber, C. Sauter, Lab Chip 9 (2009) 1412–1421.

[9] C.W. Tsao, D.L. DeVoe, Microfluid. Nanofluid. 6 (2009) 1–16.

[10] J. Greener, W. Li, J. Ren, D. Voicu, V. Pakharenko, T. Tang, E. Kumacheva, Lab Chip 10 (2010) 522–524.

[11] P. Zhou, L. Young, Z.Y. Chen, Biomed. Microdevices 12 (2010) 821–832.

[12] J.S. Jeon, S. Chung, R.D. Kamm, J.L. Charest, Biomed. Microdevices 13 (2011) 325–333.

[13] A. Alrifaiy, O.A. Lindahl, K. Ramser, Polymers-Basel 4 (2012) 1349–1398.

[14] S. Guha, S.L. Perry, A.S. Pawate, P.J.A. Kenis, Sens. Actuators B-Chem. 174 (2012) 1–9.

[15] R.K. Jena, C.Y. Yue, Y.C. Lam, Microsyst. Technol. 18 (2012) 159–166.

[16] S. Miserere, G. Mottet, V. Taniga, S. Descroix, J.L. Viovy, L. Malaquin, Lab Chip 12 (2012) 1849–1856.

[17] S. Roy, C.Y. Yue, Z.Y. Wang, L. Ananda, Sens. Actuators B-Chem. 161 (2012) 1067–1073.

[18] L.F. Peng, Y.J. Deng, P.Y. Yi, X.M. Lai, J. Micromech. Microeng. (2014) 24.

[19] H. Zhang, X.W. Liu, T. Li, X.W. Han, Micromachines-Basel 5 (2014) 1416–1428.

[20] Y. Temiz, R.D. Lovchik, G.V. Kaigala, E. Delamarche, Microelectron. Eng. 132 (2015) 156–175.

[21] F.I. Uba, B. Hu, K. Weerakoon-Ratnayake, N. Oliver-Calixte, S.A. Soper, Lab Chip 15 (2015) 1038–1049.

[22] F.I. Uba, S.R. Pullagurla, N. Sirasunthorn, J. Wu, S. Park, R. Chantiwas, Y.K. Cho, H. Shin, S.A. Soper, Analyst 140 (2015) 113–126.

[23] D.J. Guckenberger, T.E. de Groot, A.M.D. Wan, D.J. Beebe, E.W.K. Young, Lab Chip 15 (2015) 2364–2378.

[24] D.E.H. Melinda Hale, ASME 13 (2008) 5.

[25] A.S. Argon, R.E. Cohen, A.C. Patel, Polymer 40 (1999) 6991–7012.

[26] N.L. Thomas, A.H. Windle, Polymer 23 (1982) 529–542.

[27] S. Sui, Y.X. Wang, K.W. Kolewe, V. Srajer, R. Henning, J.D. Schiffman, C. Dimitrakopoulo, S.L. Perry, Lab Chip 16 (2016) 3082–3096.

[28] H. Lee, S.M. Dellatore, W.M. Miller, P.B. Messersmith, Science 318 (2007) 426–430.

[29] H. Boukellal, S. Selimovic, Y.W. Jia, G. Cristobal, S. Fraden, Lab Chip 9 (2009) 331–338.

[30] P. Garstecki, M.J. Fuerstman, H.A. Stone, G.M. Whitesides, Lab Chip 6 (2006) 437–446.

[31] M. Heymann, A. Opthalage, J.L. Wierman, S. Akella, D.M.E. Szebenyi, S.M. Gruner, S. Fraden, IUCrJ 1 (2014) 349–360.

[32] S.V. Akella, A. Mowitz, M. Heymann, S. Fraden, Cryst. Growth Des. 14 (2014) 4487–4509.

[33] L.K. Massey, Permeability Properties of Plastics and Elastomers: a Guide to Packaging and Barrier Materials, 2nd ed., Plastics Design Library/William Andrew Pub., Norwich, NY, USA, 2003.

[34] R. Seemann, M. Brinkmann, T. Pfohl, S. Herminghaus, Rep. Prog. Phys. (2012) 75.

[35] C. Holtze, A.C. Rowat, J.J. Agresti, J.B. Hutchison, F.E. Angile, C.H.J. Schmitz, S. Koster, H. Duan, K.J. Humphry, R.A. Scanga, J.S. Johnson, D. Pisignano, D.A. Weitz, Lab Chip 8 (2008) 1632–1639.